Bang *et al.*
Journal of Analytical Science and Technology (2022) 13:37
https://doi.org/10.1186/s40543-022-00347-0

Journal of Analytical Science and Technology

RESEARCH ARTICLE Open Access

High-resolution metabolomics-based biomarker discovery using exhaled breath condensate from patients with lung cancer

Geul Bang[1,2†], Ji Hyun Park[3†], Changyoung Park[1], Kwan-joong Kim[4], Jae Kwan Kim[5], Sung Yong Lee[6], Jin Young Kim[2,7*] and Youngja Hwang Park[1,4*]

Abstract

Early diagnosis and treatment are critical for improving the survival of patients with lung cancer, which is the leading cause of cancer-related deaths worldwide. In this study, we investigated whether the metabolomics analysis of exhaled breath condensate (EBC) from patients with lung cancer can provide biomarkers that can be used for noninvasive screening for lung cancer diagnosis. EBC samples obtained from patients with lung cancer ($n = 20$) and healthy individuals ($n = 5$) were subjected to high-resolution metabolomics (HRM) using liquid chromatography–mass spectrometry (LC–MS). Univariate analysis, with a false discovery rate (FDR), $q = 0.05$, and hierarchical clustering analysis were performed to discover significantly different metabolites between the healthy controls and patients with lung cancer. This was followed by the identification of the metabolites using the METLIN database. Pathway analysis based on the identified metabolites revealed that arachidonic acid (AA) metabolism was the most significantly affected pathway. Finally, 5-hydroxyicosatetraenoic acid (HETE) (*m/z* 343.2233, $[M + Na]^+$), a metabolite involved in AA metabolism, was found to be significantly higher in patients with lung cancer than in healthy counterparts. Our finding suggested that the HRM of EBC samples is a useful approach for identifying biomarkers for noninvasive screening for lung cancer diagnosis.

Keywords: Metabolomics, Exhaled breath condensate, Lung cancer, Early diagnosis, Biomarkers, Noninvasive screening

Introduction

Over the past four decades, cancer has been reported as a leading cause of morbidity and mortality in South Korea, with an estimated 210,000 new cases recorded annually and a mortality rate of 1 out 4 (Jung et al. 2015). Further, the number of deaths caused by lung cancer in South Korea increased continuously between 1983 and 2018 (Shin et al. 2020), and despite the development of several newly discovered anti-cancer drugs, lung cancer remains the leading cause of cancer-related deaths worldwide. Therefore, given the high lethality rate of lung cancer, there is a serious need for the development of diagnostic and prognostic tools for its detection at early stages.

A chest radiograph is one of the traditional tools that is used for the diagnosis of lung cancer; however, it does not offer the possibility to detect early-stage lung cancer or reduce lung cancer mortality (Oken et al. 2011; Spiro and Silvestri 2005). Further, positron emission tomography and computed tomography (PET/CT) is currently a valuable clinical oncological tool that is used in all aspects of cancer diagnosis, staging, and treatment. However, PET/CT is very expensive,

†Geul Bang and Ji Hyun Park have contributed equally to this work

*Correspondence: jinyoung@kbsi.re.kr; yjhwang@korea.ac.kr

[1] Metabolomics Laboratory, College of Pharmacy, Korea University, Sejong City 30019, Republic of Korea
[2] Research Center for Bioconvergence Analysis, Korea Basic Science Institute, Cheongju 28119, Republic of Korea
Full list of author information is available at the end of the article

and is associated with the risk of radiation exposure (Griffeth 2005; Saif et al. 2010; Spiro and Silvestri 2005). Furthermore, PET/CT has provided a false-negative finding for a lung cancer tumor with size less than 1 cm (Schrevens et al. 2004). Therefore, the identification of biomarkers is the best alternative for the early diagnosis of lung cancer and the monitoring of patients' prognosis.

Biomarkers are defined as cellular, biochemical, or molecular alterations that are measurable in biological media, such as tissues, cells, or fluids (Hulka and Wilcosky 1988). These biomarkers can be used for the diagnosis and prediction of the progression as well as the treatment outcomes of a disease in clinical practice (Mayeux 2004). Samples that can be used in this regard in relation to the lungs include bronchoalveolar lavage (BAL), sputum, peripheral blood, urine, exhaled breath gases, and exhaled breath condensate (EBC) (Grob et al. 2008). Further, specific diagnostic methods, such as BAL or bronchoscopy, with bronchial biopsy provide direct information about local airway inflammation. However, these procedures are unacceptable for routine practice as they are invasive. Although some methods, including the collection of peripheral blood or serum, are quick and minimally invasive, serum indicators may not always accurately reflect local airway inflammation. Exhaled breath is mainly analyzed via gas chromatography/mass spectrometry, which has a limitation that it offers the possibility to only analyze volatile organic compounds (Nardi-Agmon et al. 2016). EBC is a promising source of biomarkers for the detection of lung diseases (Davis et al. 2012) given that it contains various compounds that provide information regarding the physiologic and pathologic processes in the lungs (Hunt 2002). Further, as EBC contains both volatile and non-volatile compounds, including polypeptides, proteins, nucleic acids, and lipid mediators, it is more suitable for analysis aimed at discovering novel biomarkers compared to other sample types (Condensate 2006; Grob et al. 2008; Kubáň and Foret 2013). Additionally, the collection of EBC is noninvasive and easy, and it is very useful as a sample for developing self-diagnostic kits.

To discover compounds that are of significance for the noninvasive diagnosis of lung cancer, we performed metabolome analysis on EBC samples using LC–MS. Significant metabolite features were selected and pathway analysis was performed. Thus, 5-hydroxyicosatetraenoic acid (HETE) (*m/z* 343.2233, $[M+Na]^+$), one of metabolites associated with the most significantly affected pathway in lung cancer, showed potential as a biomarker for lung cancer diagnosis.

Materials and methods

Study population

The Korea University Guro Hospital Institutional review board (KUGH14273) approved this study, and informed consent was obtained from all the participants (patients and healthy individuals). A total of 25 human EBC samples were obtained from this institution, including five samples from healthy volunteers and 20 samples from patients with lung cancer. Details, such as age, height, weight, and body mass index (BMI) are provided in Table 1. From this table, it is evident that there were no significant differences between the patients with lung cancer and the health controls with respect to age, height, weight, and BMI ($p > 0.05$).

Sample collection

The EBC samples from patients with lung cancer or healthy volunteers were collected using an R-Tube, which is a sample collection device that offers the possibility to gather breath condensate in a transportable and mailable cartridge (http://respiratoryresearch.com/rtube/). Sampling was performed using a disposable 22 cm × 2.6 cm R-tube (Respiratory Research, Inc., Austin, TX, USA) encased in an aluminum cooling sleeve that was precooled to − 80 °C for at least 2 h prior to use to enable breath condensation. The subjects breathed normally through the mouthpiece for 10 min. The collection of EBC was done by closing both ends of the mouthpiece upon completion (Konstantinidi et al. 2015). Next, the samples were immediately stored at − 80 °C to prevent degradation (Carter et al. 2012), and prior to analysis via LC/MS, the thawed EBC in the R-tubes were extracted using the plunger and immediately transferred into sample vials.

Sample preparation and untargeted analysis via Quadrupole Time-of-Flight (Q-TOF) mass spectrometry

Briefly, 50-µL aliquots of the samples were first treated with 200 µL of acetonitrile followed by centrifugation

Table 1 Human EBC samples and their clinical data

Group characteristics	Healthy controls	Patients with lung cancer
Number of subjects	5	20
Sex (Male/female)	3/2	13/7
Age*	57.4 ± 7.7	66.8 ± 6.8
Height (cm) *	164.4 ± 8.73	158.24 ± 9.19
Weight (kg) *	61.8 ± 8.59	59.00 ± 11.93
BMI (kg/m^2) *	22.9 ± 2.9	23.9 ± 4.81

* Mean ± Standard Deviation (SD)

at 14,000 × *g* for 5 min at 4 °C for protein precipitation (Johnson et al. 2010). Next, the supernatant was analyzed using an ultra-performance liquid chromatography system (Agilent 1260 Infinity Quaternary, Agilent, Santa Clara, CA, USA) coupled with a Q-TOF mass spectrometry system (Agilent Q-TOF 6550, Agilent, Santa Clara, CA, USA). The analyses were performed in triplicates. The electrospray interface was operated in the positive ion mode. Further, the analysis conditions were set as follows: gas temperature, 250 °C; drying gas flow rate, 14 mL/min; nebulizer pressure, 35 psi; sheath gas temperature, 250 °C; and sheath gas flow rate, 11 mL/min (Lozano et al. 2012). Mobile phase A consisted of 0.1% formic acid in water (HPLC grade, Tedia, USA), and mobile phase B was 0.1% formic acid in acetonitrile (HPLC grade, Tedia, USA). The gradient was programmed as follows: 0–1 min, 5% (B); 1–9 min, gradient consistent to 5% (B); 9–12 min, hold at 45% (B); 12–13.5 min, 90% (B); and 13.5–13.6 min, hold at 5% (B) at a flow rate of 4 mL/min (He et al. 2016). Five microliters of each sample was first separated chromatographically using a Hypersil GOLD aQ C18 column (100 mm × 2.1 mm ID; 1.9 µm particle size, Thermo Scientific, USA) and the column heater was maintained at a temperature of 30 ℃.

Extraction of raw data and metabolic profiling via multivariate statistical analysis

Data were collected in triplicates over the 15 min elution time, and processed for the quantification of ion intensities using the R package, apLCMS, which covers a range of 50 to 1000 m/z and has a resolution of 20,000. Each feature from the triplicate LC–MS data was subsequently analyzed for m/z, retention time, and intensity. Manhattan plots were generated via bioinformatics multivariate analysis, and false discovery rates (FDRs) (Benjamini et al. 2001) were used to determine the significantly different features between the healthy controls and patients with lung cancer. Further, the R package, Limma, which originally, was used for the analysis of gene expression data arising from microarray or RNA-Seq technologies and was used in this study to compare the spectral intensities corresponding to all m/z values between healthy controls and patients (Neujahr et al. 2014; Park et al. 2015). Manhattan plots were used to visualize *p* values so as to compare the intensities of the features between the two groups after the triplicate intensities were averaged, log2 transformed, and normalized via z-transformation. The significant features obtained from the Manhattan plot were then discriminated into two groups via two-way hierarchical cluster analysis (HCA) (Uppal et al. 2013). The HCA was based on the developed agglomerative clustering method, and it revealed significant m/z values and sample hierarchies, with each cluster branch comprising similar groups that can be used to differentiate between the m/z values corresponding to the healthy controls and patients with lung cancer (žurauskiene and Yau 2016). Manhattan plots and HCA analysis were performed using xmsPANDA package.

Data annotation and pathway analysis

The significant features were annotated based on m/z values, name, formula, and Kyoto Encyclopedia of Genes and Genomes (KEGG) ID using the METLIN metabolite database. An m/z error tolerance value of ± 20 ppm was used. Further, pathway analysis was performed based on KEGG, and the given KEGG ID was used to map the features on the KEGG pathway. Furthermore, detected features in KEGG were queried into the human metabolic pathway (Ogata et al. 1998) and MetaboAnalyst (http://www.metaboanalyst.ca), and the detected features that matched known human intermediary metabolites were then presented as black dots in a map. MetaboAnalyst pathway topological analysis uses relative centrality and outdegree centrality values to calculate the importance of each compound. Additionally, the sum of the importance measures of all the metabolites in each pathway yielded the pathway impact as the sum of the importance measures matching the normalized metabolites. Using MetaboAnalyst, a number of univariate analyses, including t test were performed at the compound level to provide a detailed view of the distribution of the concentrations of the individual metabolites with regard to phenotypes (Xia et al. 2011). In this study, after searching the METLIN database, the KEGG number was applied to the pathway analysis in MetaboAnalyst. Thus, we obtained an overview of the pathway as well as detail information regarding the pathway. Additionally, significant features were catalogued for specificity and accuracy using a receiver operating characteristic (ROC) curve obtained using MedCalc software. (Schoonjans et al. 1995).

Results and discussion

Metabolomics-wide associated study (MWAS)

Figure 1 presented the scheme showing the experimental procedure. Metabolites were extracted from each EBC sample and followed by the analysis using high-resolution LC–MS. Then, a MWAS and pathway analysis were conducted to identify potential lung cancer biomarkers. Metabolomics differences between the healthy controls and patients with lung cancer were determined by generating a Manhattan plot, which utilizes statistical tests to select significantly different metabolites between cancer patients relative to healthy controls. In the Manhattan plot, the x-axis represents the m/z range (50–1000), while the y-axis represents

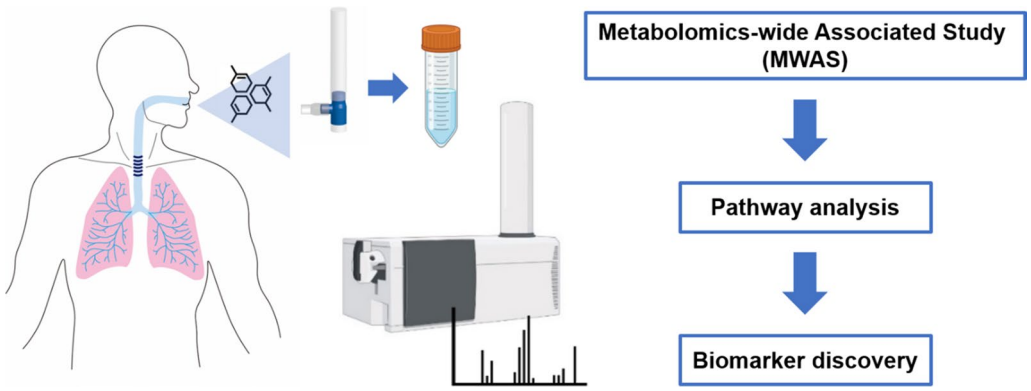

Fig. 1 Scheme showing the experimental procedure

the –log10 value of the raw *p*-value, and the dashed line represents the FDR significant level. Therefore, any m/z above this line was significantly different for the patients and controls at FDR, q = 0.05. Thus, comparing the healthy controls ($n = 5$) and the patients with lung cancer ($n = 25$), a total of 344 significantly different features were observed (green dots in Fig. 2a). Further, two-way HCA (Fig. 2b) showed clearly divided metabolite expression into two branches, one for the controls (red bar) and the other for the patients with lung cancer (green bar).

Pathway analysis using KEGG and MetaboAnalyst

Significant features were annotated in the METLIN database considering positive ion adducts within a mass accuracy of 20 ppm. After METLIN data processing, the KEGG numbers of the identified metabolites were obtained and applied to the human metabolic KEGG pathway analysis as well as MetaboAnalyst.

KEGG pathway analysis showed 89 significant features indicated by the black dots in Fig. 3. From this figure, it was evident that the most affected KEGG pathway was arachidonic acid (AA) metabolism, with 19 hits followed

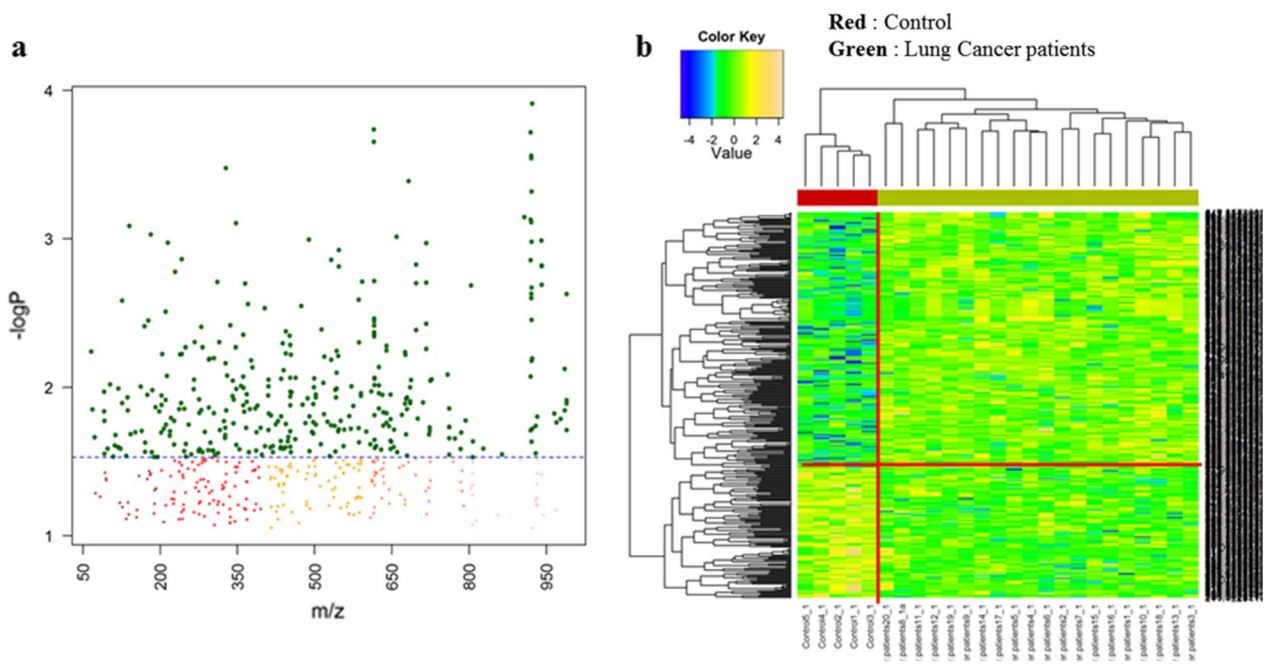

Fig. 2 Manhattan plot and hierarchical cluster analysis (HCA) plot. **A** Manhattan plot. The blue dotted line corresponds to q = 0.05 comparing the healthy controls ($n = 5$) with patients with lung cancer ($n = 20$), while the green dots above the blue line represent significantly different compounds. **B** HCA analysis using significantly different features between the healthy controls (Red) and patients with lung cancer (Green)

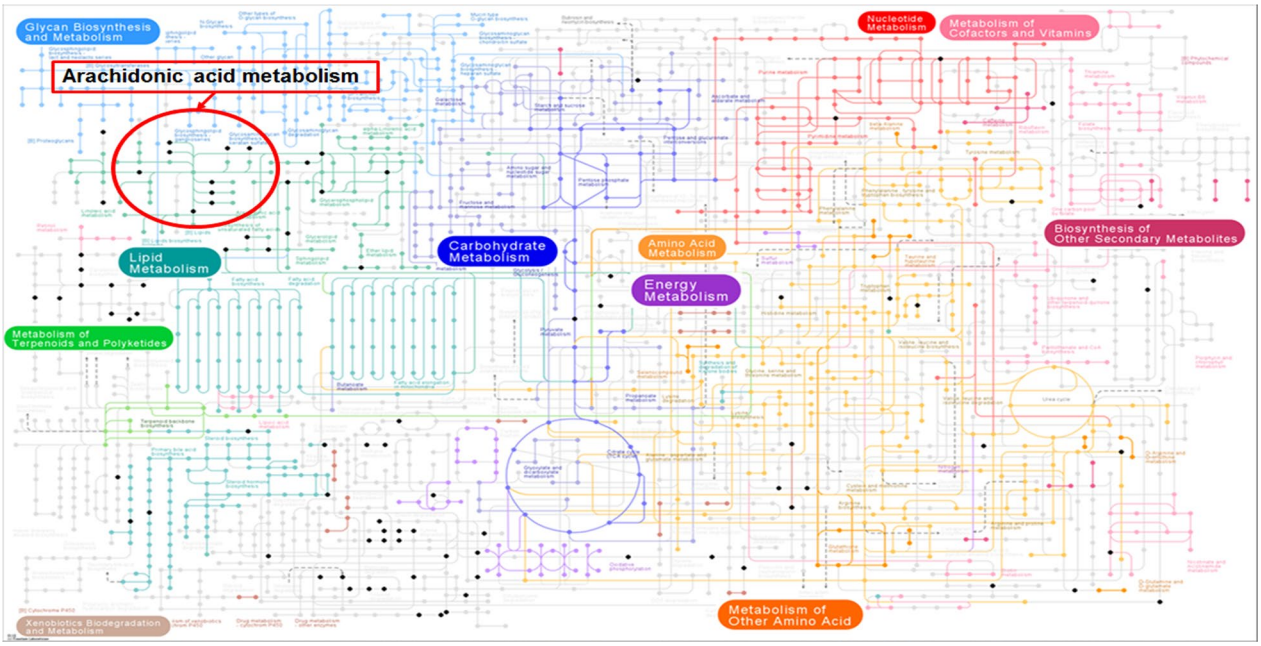

Fig. 3 Kyoto Encyclopedia Genes and Genomics (KEGG) pathway analysis. In total, the KEGG map comprised 89 black dots representing detected features that matched known human intermediary metabolites. The most affected KEGG pathway was arachidonic acid metabolism

Table 2 Top 9 affected KEGG pathways with five and more compound hits

Top 9 affected KEGG pathways	Compound hits
Arachidonic acid metabolism	19
Glycerophospholipid metabolism	7
Ubiquinone and other terpenoid quinone biosynthesis	7
Tyrosine metabolism	6
Inflammatory mediator regulation of TRP channels	6
Bile secretion	6
Serotonergic synapse	6
Sphingolipid metabolism	5
Phenylalanine metabolism	5

by glycerophospholipid metabolism with 7 hits (Table 2 and Fig. 3).

Next, via MetaboAnalyst, we obtained potential target pathways with pathway impact values calculated via pathway topology analysis. The impact values of AA metabolism, limonene and pinene degradation, sphingolipid metabolism, and lysine biosynthesis were 0.153, 0.224, 0.324, and 0.209, and their –log(p) values were 3.004, 2.608, 1.852, and 0.304, respectively, as shown in Table 3 and Fig. 4.

Pathway analysis using KEGG and MetaboAnalyst commonly showed that AA metabolism was the most

Table 3 Pathway analysis with 89 significantly different metabolites using MetaboAnalyst

Pathway Name	Total	Hits	− log(p)	Impact
Arachidonic acid metabolism	62	12	3.004	0.153
Limonene and pine degradation	59	11	2.608	0.224
Sphingolipid metabolism	59	11	1.852	0.324
Lysine biosynthesis	32	3	0.304	0.209

affected pathway, with the highest number of hits in the HRM of EBC from health controls and patients with lung cancer. AA is a long-chain polyunsaturated fatty acid present in cell membranes. Its metabolism by cyclooxygenase and lipoxygenase generates eicosanoids, such as prostaglandins, thromboxanes, and leukotrienes, which are primarily pro-inflammatory and promote carcinogenesis by modulating tumor cell proliferation, differentiation, apoptosis, and angiogenesis (Larsson et al. 2004). Since the AA metabolism pathway produces a variety of bioactive metabolites, it has been addressed as important in various diseases, including cancer and inflammation (Tapiero et al. 2002). Studies on the mechanisms and biology of lung cancer have suggested that the metabolites including prostanoids, leukotrienes (LTs), epoxyeicosatrienoic acids (EETs), dihydroxyeicosatetraenoic acid (diHETEs), eicosatetraenoic acids (ETEs), and lipoxins (LXs) of AA metabolism could play an important role in

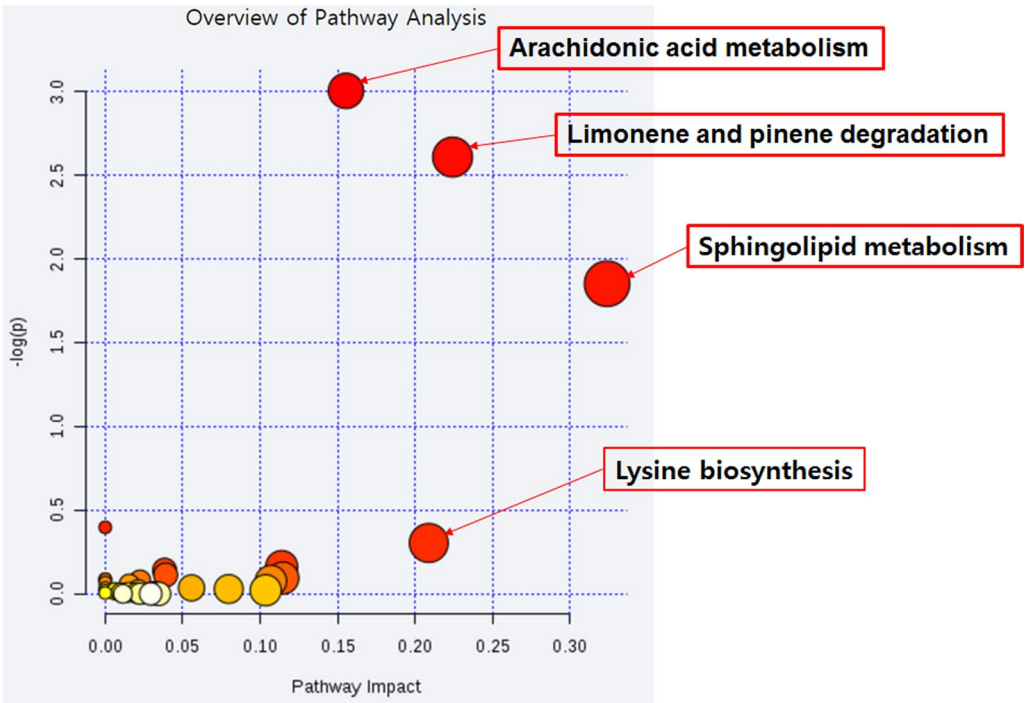

Fig. 4 Pathway identification results with 89 significantly different metabolites using MetaboAnalyst. (healthy controls vs. patients with lung cancer). Pathway impact value (x-axis) from pathway topology analysis and *p*-values from pathway enrichment analysis (y-axis) are shown

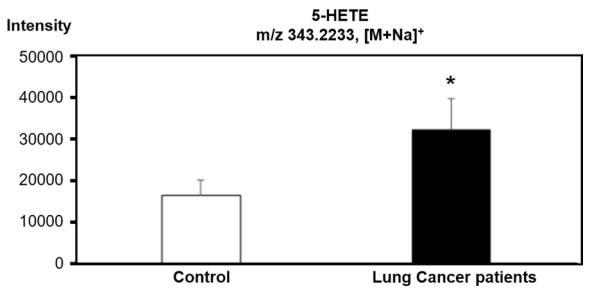

Fig. 5 Bar graph of intensities of 5-HETE (*m/z* 343.2233, $[M+Na]^+$) in EBC samples from healthy controls and patients with lung cancer. (*p* values < 0.05)

lung cancer pathogenesis (Stearman et al. 2007; Wang et al. 2021).

Identification of novel biomarker and ROC curve

We noted that among the metabolites involved in AA metabolism, 5-hydroxyicosatetraenoic (HETE) showed a higher level in patients with lung cancer than in the healthy controls (Fig. 5). In our high-resolution LC–MS analysis, the compounds expected to be 5-HETE were detected in 20 out of 25 EBC samples with average molecular ion at m/z 343.2233 and average retention time at 11.77 min. The molecular weight was identified within 3.2 ppm mass tolerance to theoretical molecular weight of 5-HETE of $[M+Na]^+$ (m/z 343.2244). When compared with LC–MS analysis results of 5-HETE standards, it gave the identical results as the compounds detected in EBC samples with difference of 0.6 min retention time and 2.0 ppm mass tolerance (Additional file 1: Fig. S1).

A previous study (Liu et al. 2014) revealed that 5-HETE, 11-HETE, 12-HETE, and 15-HETE are 1.8- to 3.3-fold higher in sera samples from patients with lung cancer than in samples from healthy individuals.

5-HETE has been identified as a biologically important and active lipid compound that plays a role in the pathogenesis of human lung cancer, and blocking its biosynthesis significantly inhibits the proliferation of epithelial lung cancer cells in vitro and in vivo (Avis et al. 1996; Hong et al. 1999; Paige et al. 2009). It has also been reported that 5-HETE plays a role in promoting the growth of prostate, breast, and pancreatic cancer cells. (Avis et al. 2001; Ding et al. 2003; Ghosh and Myers 1998).

Figure 6 shows the ROC curve of 5-HETE, highlighting it as potential biomarker compound for lung cancer diagnosis. The area under the curve (AUC) of the ROC curve, sensitivity, and specificity were 0.633, 45%, and 87%, respectively. Although the sensitivity was relatively low, PSA, a prostate cancer biomarker currently used in

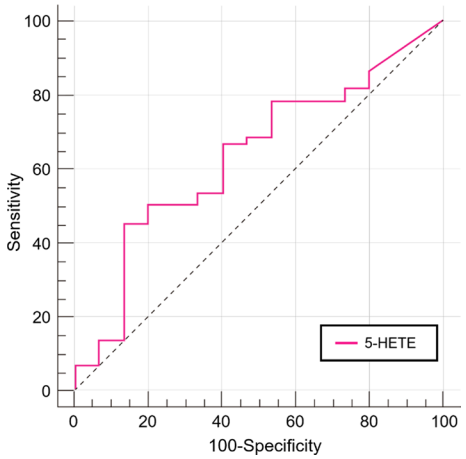

Fig. 6 Receiver operating characteristic (ROC) curves for 5-HETE (*m/z* 343.2233, $[M+Na]^+$) as potential biomarker for distinguishing healthy controls and patients with lung cancer. The x-axis represents 100-specificity, while the y-axis represents sensitivity

the clinic, also presents a similar level of sensitivity and specificity of 45% and 91%, respectively (Polanski and Anderson 2006).

Conclusion

To develop biomarkers for noninvasive screening for lung cancer diagnosis, we performed metabolomics analysis on EBC. Thus, we observed significant metabolites that discriminated healthy controls and patients with lung cancer and identified AA metabolism as the most affected pathway. Our results also showed that the level of 5-HETE, one of the metabolites involved in the AA metabolism pathway, was significantly increased in patients with lung cancer patients compared with its level in samples from healthy controls. Further, as a biomarker of lung cancer, 5-HETE showed an AUC value (ROC) of 0.633 and a specificity of 86.67.

Given that our analysis involved a limited number of samples, additional experiments are required to validate these results regarding the usefulness of 5-HETE. Nevertheless, our results showed that EBC is a useful noninvasive clinical sample for biomarker discovery in lung disease and that metabolite analysis is an efficient approach for biomarker discovery.

Abbreviations

HRM: High-resolution metabolomics; EBC: Exhaled breath condensate; LC–MS: Liquid chromatography–mass spectrometry; FDR: False discovery rate; HCA: Hierarchical clustering analysis; AA: Arachidonic acid; HETE: 5-Hydroxyicosatetraenoic acid; PET/CT: Positron emission tomography/computed tomography; BMI: Body mass index; KEGG: Kyoto encyclopedia of genes and genomes; ROC curves: Receiver operating characteristic curves; AUC: Area under the curve.

Supplementary Information

The online version contains supplementary material available at https://doi.org/10.1186/s40543-022-00347-0.

Additional file 1: Fig. S1. The chromatogram and the high-resolution mass spectrum of 5-HETE standard.

Acknowledgements

None

Author contributions

YHP and JYK contributed to conceptualization, methodology, and project administration. GB and JHP conducted metabolomics, formal analysis, writing—the original draft, and writing—revision of the manuscript. CP adjusted the figures and wrote the manuscript. KK and JKK contributed additional metabolomics and the relevant figure reconstruction in the revision. SYL collected samples and provided professional advice. All authors contributed to the manuscript review and approved the submitted version.

Funding

This work was supported by a National Research Foundation of Korea Grant funded by the Korean government (MSIT) (Grant No.: NRF-2020R1A2C2103067) and the Research Program funded by the National Research Council of Science & Technology (CRC22021-100).

Availability of data and materials

All the data are available based on request.

Declarations

Competing interests

The authors declare that they have no competing interests.

Author details

[1]Metabolomics Laboratory, College of Pharmacy, Korea University, Sejong City 30019, Republic of Korea. [2]Research Center for Bioconvergence Analysis, Korea Basic Science Institute, Cheongju 28119, Republic of Korea. [3]College of Pharmacy, Duksung Women's University, Seoul 01370, Republic of Korea. [4]Omics Research Center, Sejong 30019, Republic of Korea. [5]Seoul Center, Korea Basic Science Institute, Seoul 02841, Republic of Korea. [6]Division of Pulmonary, Allergy, and Critical Care Medicine, Korea University Guro Hospital, Seoul 08308, Republic of Korea. [7]Critical Diseases Diagnostics Convergence Research Center, Korea Research Institute of Bioscience and Biotechnology, Daejeon 34141, Republic of Korea.

Received: 10 August 2022 Accepted: 12 October 2022
Published online: 18 October 2022

References

Avis IM, Jett M, Boyle T, Vos MD, Moody T, Treston AM, et al. Growth control of lung cancer by interruption of 5-lipoxygenase-mediated growth factor signaling. J Clin Invest. 1996;97(3):806–13.

Avis I, Hong SH, Martínez A, Moody T, Choi YH, Trepel J, et al. Five-lipoxygenase inhibitors can mediate apoptosis in human breast cancer cell lines through complex eicosanoid interactions. FASEB J. 2001;15(11):2007–9.

Benjamini Y, Drai D, Elmer G, Kafkafi N, Golani I. Controlling the false discovery rate in behavior genetics research. Behav Brain Res. 2001;125(1–2):279–84.

Carter SR, Davis CS, Kovacs EJ. Exhaled breath condensate collection in the mechanically ventilated patient. Respir Med. 2012;106(5):601–13. https://doi.org/10.1016/j.rmed.2012.02.003.

Condensate B. ATS workshop proceedings: Exhaled nitric oxide and nitric oxide oxidative metabolism in exhaled breath condensate: executive summary. Am J Respir Crit Care Med. 2006;173(7):811–3.

Davis MD, Montpetit A, Hunt J. Exhaled Breath Condensate. Immunol Allergy Clin North Am. 2012;32(3):363–75. https://doi.org/10.1016/j.iac.2012.06.014.
Ding XZ, Tong WG, Adrian TE. Multiple signal pathways are involved in the mitogenic effect of 5(S)-HETE in human pancreatic cancer. Oncology. 2003;65(4):285–94.
Ghosh J, Myers CE. Inhibition of arachidonate 5-lipoxygenase triggers massive apoptosis in human prostate cancer cells. Proc Natl Acad Sci U S A. 1998;95(22):13182–7.
Griffeth LK. Use of Pet/Ct scanning in cancer patients: technical and practical considerations. Baylor Univ Med Cent Proc. 2005;18(4):321–30.
Grob NM, Aytekin M, Dweik RA. Biomarkers in exhaled breath condensate: A review of collection, processing and analysis. J Breath Res. 2008. https://doi.org/10.1088/1752-7155/2/3/037004.
He Z, Xu Y, Wang L, Peng Y, Luo M, Cheng H, et al. Wide-scope screening and quantification of 50 pesticides in wine by liquid chromatography/quadrupole time-of-flight mass spectrometry combined with liquid chromatography/quadrupole linear ion trap mass spectrometry. Food Chem. 2016;196:1248–55. https://doi.org/10.1016/j.foodchem.2015.10.042.
Hong SH, Avis I, Michele DV, Martínez A, Treston AM, Mulshine JL. Relationship of arachidonic acid metabolizing enzyme expression in epithelial cancer cell lines to the growth effect of selective biochemical inhibitors. Cancer Res. 1999;59(9):2223–8.
Hulka BS, Wilcosky T. Biological markers in epidemiologic research. Arch Environ Health. 1988;43(2):83–9.
Hunt J. Exhaled breath condensate: An evolving tool for noninvasive evaluation of lung disease. J Allergy Clin Immunol. 2002;110(1):28–34. https://doi.org/10.1067/mai.2002.124966.
Johnson JM, Yu T, Strobel FH, Jones DP. A practical approach to detect unique metabolic patterns for personalized medicine. Analyst. 2010;135(11):2864–70.
Jung KW, Won YJ, Kong HJ, Oh CM, Cho H, Lee DH, et al. Cancer statistics in Korea: incidence, mortality, survival, and prevalence in 2012. Cancer Res Treat. 2015;47(2):127–41.
Konstantinidi EM, Lappas AS, Tzortzi AS, Behrakis PK. Exhaled Breath condensate: technical and diagnostic aspects. Sci World J. 2015;2015.
Kubáň P, Foret F. Exhaled breath condensate: determination of non-volatile compounds and their potential for clinical diagnosis and monitoring. A Review Anal Chim Acta. 2013;805:1–18.
Larsson SC, Kumlin M, Ingelman-Sundberg M, Wolk A. Dietary long-chain n-3 fatty acids for the prevention of cancer: a review of potential mechanisms. Am J Clin Nutr. 2004;79(6):935–45.
Liu J, Mazzone PJ, Cata JP, Kurz A, Bauer M, Mascha EJ, et al. Serum free fatty acid biomarkers of lung cancer. Chest. 2014;146(3):670–9.
Lozano A, Martínez-Uroz MA, Gómez-Ramos MJ, Gómez-Ramos MM, Mezcua M, Fernández-Alba AR. Determination of nicotine in mushrooms by various GC/MS- and LC/MS-based methods. Anal Bioanal Chem. 2012;402(2):935–43.
Mayeux R. Biomarkers: potential uses and limitations. NeuroRx. 2004;1(2):182–8.
Nardi-Agmon I, Abud-Hawa M, Liran O, Gai-Mor N, Ilouze M, Onn A, et al. Exhaled breath analysis for monitoring response to treatment in advanced lung cancer. J Thorac Oncol. 2016;11(6):827–37.
Neujahr DC, Uppal K, Force SD, Fernandez F, Lawrence C, Pickens A, et al. Bile acid aspiration associated with lung chemical profile linked to other biomarkers of injury after lung transplantation. Am J Transplant. 2014;14(4):841–8.
Ogata H, Goto S, Fujibuchi W, Kanehisa M. Computation with the KEGG pathway database. BioSystems. 1998;47(1–2):119–28.
Oken MM, Hocking WG, Kvale PA, Andriole GL, Buys SS, Church TR, et al. Screening by chest radiograph and lung cancer mortality: the prostate, lung, colorectal, and ovarian (PLCO) randomized trial. JAMA J Am Med Assoc. 2011;306(17):1865–73.
Paige M, Saprito MS, Bunyan DA, Shim YM. HPLC quantification of 5-hydroxyeicosatetraenoic acid in human lung cancer tissues. Biomed Chromatogr. 2009;23(8):817–21.
Park YH, Shi YP, Liang B, Medriano CAD, Jeon YH, Torres E, et al. High-resolution metabolomics to discover potential parasite-specific biomarkers in a Plasmodium falciparum erythrocytic stage culture system. Malar J. 2015;14(1):1–9.
Polanski M, Anderson NL. A list of candidate cancer biomarkers for targeted proteomics. Biomark Insights. 2006;1(301):117727190600100.
Saif MW, Tzannou I, Makrilia N, Syrigos K. Role and cost effectiveness of PET/CT in management of patients with cancer. Yale J Biol Med. 2010;83(2):53–65.
Schoonjans F, Zalata A, Depuydt CE, Comhaire FH. MedCalc: a new computer program for medical statistics. Comput Methods Programs Biomed. 1995;48(3):257–62.
Schrevens L, Lorent N, Dooms C, Vansteenkiste J. The role of PET scan in diagnosis, staging, and management of non-small cell lung cancer. Oncologist. 2004;9(6):633–43.
Shin HY, Kim J, Lee S, Park MS, Park S, Huh S. Cause-of-death statistics in 2018 in the Republic of Korea. J Korean Med Assoc. 2020;63(5):286–97.
Spiro SC, Silvestri GA. One hundred years of lung cancer. Am J Respir Crit Care Med. 2005;172(5):523–9.
Stearman RS, Grady MC, Nana-Sinkam P, Varella-Garcia M, Geraci MW. Genetic and epigenetic regulation of the human prostacyclin synthase promoter in lung cancer cell lines. Mol Cancer Res. 2007;5(3):295–308.
Tapiero H, Nguyen Ba G, Couvreur P, Tew KD. Polyunsaturated fatty acids (PUFA) and eicosanoids in human health and pathologies. Biomed Pharmacother. 2002;56(5):215–22.
Uppal K, Soltow QA, Strobel FH, Pittard WS, Gernert KM, Yu T, et al. XMSanalyzer: Automated pipeline for improved feature detection and downstream analysis of large-scale, non-targeted metabolomics data. BMC Bioinform. 2013. https://doi.org/10.1186/1471-2105-14-15.
Wang B, Wu L, Chen J, Dong L, Chen C, Wen Z, et al. Metabolism pathways of arachidonic acids: mechanisms and potential therapeutic targets. Signal Transduct Target Ther. 2021. https://doi.org/10.1038/s41392-020-00443-w.
Xia J, Wishart DS, Valencia A. MetPA: a web-based metabolomics tool for pathway analysis and visualization. Bioinformatics. 2011;27(13):2342–4.
Žurauskiene J, Yau C. pcaReduce: Hierarchical clustering of single cell transcriptional profiles. BMC Bioinform. 2016;17(1):1–11. https://doi.org/10.1186/s12859-016-0984-y.

Publisher's Note